Thermodynamic studies on single-crystalline Gd_2BaNiO_5

E. A. Popova,[1] R. Klingeler,[2] N. Tristan,[3] B. Büchner,[3] and A. N. Vasiliev[4,*]

[1]*Moscow State Institute of Electronics and Mathematics (Technical University), 109028 Moscow, Russia*

[2]*Kirchhoff Institute for Physics, University of Heidelberg, INF 227 69120, Heidelberg, Germany*

[3]*Leibniz-Institute for Solid State and Materials Research IFW Dresden, 01171 Dresden, Germany*

[4]*Low Temperature Physics and Superconductivity Department, Moscow State University, 119991 Moscow, Russia*

(Received 22 October 2011; revised manuscript received 10 February 2012; published 2 May 2012)

We present the thermodynamic properties and the magnetic phase diagram of Gd_2BaNiO_5 investigated by means of specific heat and magnetization measurements performed along the main crystallographic axes of the single crystal. Our data imply antiferromagnetic ordering at $T_N = 55$ K and a spontaneous spin-reorientation transition at $T_{SR} = 24$ K. Upon application of external magnetic fields, a spin-flop transition is observed at $T < T_{SR}$ in magnetic fields $B \parallel b$ axis and at $T_{SR} < T < T_N$ in magnetic fields $B \parallel a$ axis. The magnetic phase diagram in Gd_2BaNiO_5 is established from these data. Considering Gd-Gd and Gd-Ni interactions allows estimating the magnetic contribution of the gadolinium subsystem to the magnetization and the specific heat. The Gd-Gd interaction is organized via Ni chains being therefore sensitive to the angle between Gd and Ni magnetic moments. The analysis of the experimental data shows that the behavior of the nickel subsystem differs from that of a classical antiferromagnet.

DOI: 10.1103/PhysRevB.85.174402 PACS number(s): 75.30.Kz, 75.40.Cx, 75.10.Pq

I. INTRODUCTION

Magnetism in low-dimensional systems is a fundamentally relevant phenomenon where quantum effects may cause novel and intriguing ground states with unusual excitations. A famous example is the antiferromagnetic spin chain with integer spin, i.e., Haldane chain, where a gap in the elementary excitation spectrum appears.[1,2] The magnetic subsystem in Y_2BaNiO_5 excellently realizes such a one-dimensional system with negligible interactions between the chains of integer spin $S = 1$ at the Ni^{2+} ion sites, which are almost isotropically coupled by antiferromagnetic exchange interactions. Structurally, R_2BaNiO_5 (R = rare-earth or yttrium) contains flattened corner-sharing NiO_6 octahedra, which form infinite chains along the a axis interconnected through R^{3+} and Ba^{2+} ions.[3] Indeed, there is no long range magnetic order in Y_2BaNiO_5 down to at least 0.1 K[4] and a singlet ground state is confirmed by neutron and magnetization studies, which imply a Haldane gap of about 10 meV in the magnetic excitation spectrum.[5,6] In addition, the family of R_2BaNiO_5 allows studying the borderline between quantum and classical magnetism by introducing magnetic rare-earth ions at the R-sites. This yields a subsystem of rather classical spins weakly coupled to the $S = 1$ antiferromagnetic Haldane chains.[3] Interestingly, depending on the actual rare-earth ion, long range antiferromagnetic order appears in the range $10 \div 50$ K,[7–10] which yields an effective staggered field acting on the $S = 1$ chains. Since there is only weak direct coupling between the rare-earth moments, the interaction is necessarily mediated by the Ni chains. The anisotropy of the rare-earth ions causes the orientation of the magnetic moments of both Ni^{2+} and R^{3+} ions. On the other hand, clear signatures of the quantum ground state are still observed since polarized and unpolarized inelastic neutron scattering experiments on R_2BaNiO_5 have shown the paradoxical coexistence of Haldane-gap excitations and spin waves, i.e., of classical and quantum spin dynamics, in the ordered state.[11–13]

In Gd_2BaNiO_5, the R-sites are occupied by Gd^{3+}-ions with half-filled f-shells, i.e., $S = 7/2$. It crystallizes in the orthorhombic space group *Immm*.[14,15] Observation of the magnetic superstructure in the ordered state by means of neutron diffraction has not yet been successful due to the high absorption cross section of natural Gd. However, infrared optical spectroscopy[16] and Mössbauer spectroscopy[17] enable us to conclude that Gd_2BaNiO_5 orders antiferromagnetically at $T_N = 53$ K and undergoes a spin-reorientation transition at $T_{SR} = 24$ K. The temperature dependencies of the magnetic susceptibility taken along the a and b axes, respectively, indicate a Curie-Weiss-like behavior above T_N.[18] However, a detailed analysis of these dependences and of the magnetic phase diagram below T_N is missing and, at present, the behavior of the Ni subsystem, which is supposed to be intrinsically disordered even below T_N, has not been analyzed.

In this work the thermodynamic properties of a Gd_2BaNiO_5 single crystal are investigated by means of detailed magnetization and specific heat measurements performed in different orientations of the magnetic field with respect to the crystallographic axes. The magnetic susceptibility and specific heat data confirm antiferromagnetic ordering and spontaneous spin reorientation found by previous optical and Mössbauer studies.[16,17] Our measurements allow us to establish the anisotropic magnetic phase diagram. In particular, a spin-flop transition is observed at $T < T_{SR}$ in a magnetic field $B \parallel b$ axis and at $T_{SR} < T < T_N$ in a magnetic field $B \parallel a$ axis. Analyzing both the specific heat and the magnetization data demands considering both the Gd-Gd and the Gd-Ni interactions, which allow a quantitative estimate of the respective contributions due to the gadolinium subsystem. Our analysis implies that the behavior of the nickel subsystem differs from the behavior of the ordered spins in an antiferromagnet.

II. EXPERIMENTAL

A Gd_2BaNiO_5 single crystal was grown by the travelling-solvent floating-zone technique, as described in Ref. 19. The static magnetization $M(T)$ was measured in a magnetic field of $B = 0.05$ T in the temperature range 1.8–350 K using a

MPMS-XL5 SQUID magnetometer (Quantum Design). The field dependence of the magnetization $M(B)$ was measured at temperatures 4.2 ÷ 120 K in magnetic fields up to 15 T by means of a home-built vibrating sample magnetometer (VSM).[20] The field sweep rate was approximately 0.2 T/min. The specific heat was studied in the temperature range 1.8 ÷ 300 K in magnetic fields of 0, 1, and 2 T, respectively, oriented along the b axis of the crystal by means of a relaxation method in the Physical Property Measurement System (Quantum Design).

A. Experimental results

The evolution of long range spin order in Gd_2BaNiO_5 and the associated phase transitions yield pronounced anomalies in the magnetization and specific heat data (Fig. 1). In the specific heat in Fig. 1(b) there is a jumplike or weakly λ-type anomaly at $T_N = 55$ K, which signals the onset of long range magnetic order by means of a second-order phase transition. The sharp anomaly at $T_{SR} = 24$ K implies a discontinuous phase transition associated with spontaneous spin reorientation. Both temperatures are in good agreement with the optical and Mössbauer spectroscopy data in Refs. 16 and 17. In addition, there is a broad hump in the specific heat data at $T \approx 20$ K. This feature is indicative of a Schottky anomaly, which reveals the temperature-driven repopulation of the ground state of the Gd^{3+} ions split in the internal magnetic field in the ordered state associated with the ordered state.

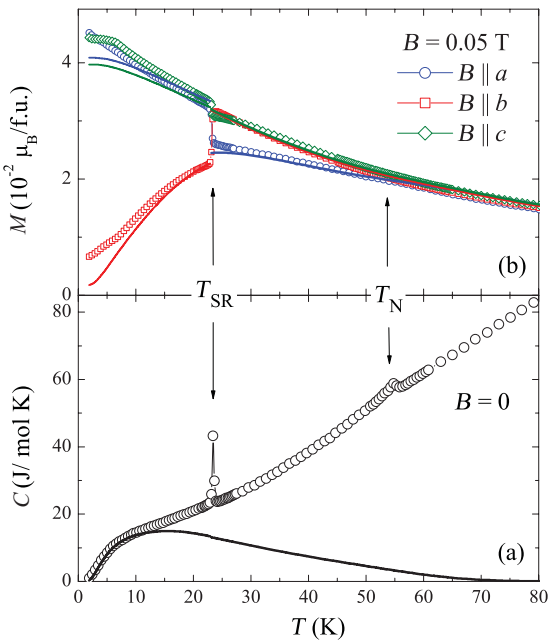

FIG. 1. (Color online) (a) Temperature dependences of the magnetization M measured along the different crystallographic axes in an external magnetic field of $B = 0.05$ T. (b) The temperature dependence of the specific heat $C(T)$ measured in zero magnetic field in the temperature range 2–100 K. In both plots experimental data are shown by open symbols, and solid lines display the contribution of the Gd subsystem (see the text). T_N and T_{SR} mark the onset of long range antiferromagnetic order and the spin-reorientation transition, respectively.

Quantitatively, the specific heat jump at T_N amounts to $\Delta C = 2.4$ J/(mol·K). This value does *not* agree with the calculated jump $\Delta C = \frac{5S(S+1)}{S^2+(S+1)^2}R$ (R is the gas constant) predicted by mean field theory for antiferromagnetic spin order.[21] To be specific, the mean field theory predicts $\Delta C_{Ni} = 16.6$ J/(mol·K) for the Ni^{2+} ($S = 1$) subsystem and $\Delta C_{Gd} = 40.3$ J/(mol·K) for the Gd^{3+} ($S = 7/2$) one. The data hence imply either strong spin disorder and/or the reduction of the magnetic moments caused by quantum spin fluctuations below T_N or the presence of significant spin correlations which yield a release of entropy already well above the Neel temperature. We suppose that both effects are relevant. There is indeed experimental evidence for spin disorder at $T < T_N$ since spin orientation at T_{SR} is associated with entropy changes, too, presumably mainly of magnetic nature. These discontinuous entropy changes amount to $\Delta S_{SR} = 0.37$ J/(mol·K).

In Fig. 1(a) the temperature dependencies of the magnetization $M_a(T)$, $M_b(T)$, and $M_c(T)$ measured along the crystallographic a, b, and c axes, respectively, are displayed. While above $T \approx 100$ K, as shown in Fig. 2, the magnetization measured in different directions is almost isotropic, there is a significant anisotropy of the magnetic properties below the Neel temperature. However, the data display no clear anomaly at T_N. At $T < T_N$, the magnetization M_a measured along the a axis is smaller than M_b and M_c measured along the b and c axes, respectively. The discontinuous transition at T_{SR} is indicated by a pronounced jump in the magnetization. The data imply, upon cooling, magnetization jumps at 0.05 T of $\Delta M(B||a) = 5.9 \times 10^{-2}\,\mu_B$/f.u., $\Delta M(B||b) = -8.7 \times 10^{-2}\,\mu_B$/f.u., and $\Delta M(B||c) = 2.4 \times 10^{-2}\,\mu_B$/f.u. for the different field directions. We note a small kink in χ_b(T) and χ_c(T) at $T = 7$ K.

In order to establish the magnetic phase diagram, the field dependences of the magnetization $M_a(B)$, $M_b(B)$, and $M_c(B)$ were measured along the a, b, and c axes at various temperatures. These dependences taken at $T = 4.2$ K and $T = 30$ K are shown in Fig. 3. Above $B \sim 5$ T, all magnetization curves have a nonlinear character with a negative curvature, i.e., the magnetization curves are bent to the right. M_a is larger

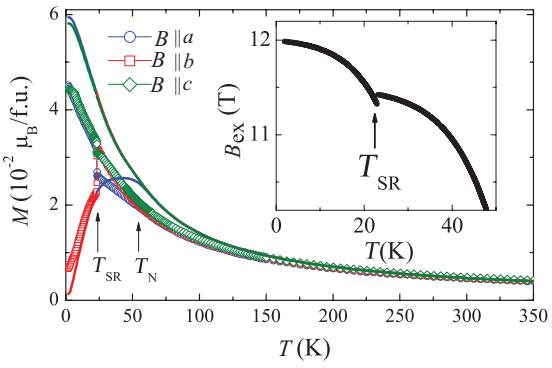

FIG. 2. (Color online) Temperature dependence of the magnetization M measured along the a, b, and c axes, respectively, in an external magnetic field of $B = 0.05$ T. Experimental data are shown by open symbols. Solid lines show the contribution of the Gd subsystem for the case of negligible Gd-Gd and Gd-Ni interactions. Inset: Temperature dependence of the internal magnetic field B_{ex} acting on the Gd^{3+} moments (see the text).

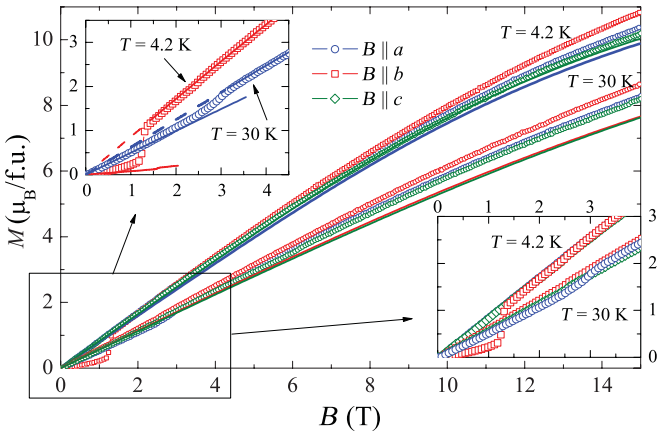

FIG. 3. (Color online) Field dependences of the magnetization $M_a(B)$, $M_b(B)$, and $M_c(B)$ measured along the a, b, and c axes, respectively, at $T = 4.2$ K and $T = 30$ K. Lower inset: $M_a(B)$ and $M_b(B)$ in small fields. Upper inset: $M_a(B)$ at $T = 30$ K and $M_b(B)$ at $T = 4.2$ K where the spin-flop transition is observed. Experimental data are shown by open symbols; solid lines show the contribution of Gd subsystem.

than M_b and M_c but there is very similar field dependence in the high field range. In contrast, there is a strong anisotropy below $B \sim 5$ T if the field is applied along the a or b axes. This becomes visible in more detail by the magnetization curves $M(B\|a)$ and $M(B\|b)$, shown in Fig. 4. The main features in the curves are jumps in the magnetization, which are present at temperatures below $T_{SR} = 24$ K in magnetic fields $B \parallel b$ axis and at $T_{SR} < T < T_N$ for $B \parallel a$ axis. It is straightforward to attribute these features with a spin-floplike field-driven reorientation of the spins. There are clear maxima in the derivatives $\partial M/\partial B$, which enable us to identify the corresponding critical fields B_C, e.g., $B_C(T = 4.2\ \text{K}) \parallel b = 1.25$ T. A tiny hysteresis indicates the first-order character of the spin-flop transition. At intermediate fields there is a quasilinear field dependence of the magnetization which extrapolates to $M(B = 0) = 0$ as expected for a spin-flop transition [cf. dashed line in Fig. 4(a)]. Upon heating the jump in $M(B\|b)$ reduces in size. Concomitantly, the critical field B_C increases with increasing the temperature up to $T \approx 14$ K and then decreases and eventually vanishes at T_{SR}. In contrast, there is no such feature in $M(B\|a)$ for temperatures below T_{SR}, but it appears at $T_{SR} < T < T_N$. Again, the jump ΔM reduces and smoothes upon heating, and the critical field B_C shifts towards higher fields with increasing the temperature up to T_N. The spin-flop transition is absent above T_N as well as for magnetic fields applied along the c axis.

This behavior is summarized in the magnetic phase diagram in Fig. 5. Here, the effect of external magnetic fields applied $\|b$ axis (full symbols) and $\|$ a axis (open symbols) is merged. Clearly, two separate regimes are visible. The phase boundaries meet at $T_{SR}(B = 0)$ where the first-order spin-reorientation transition is associated with both entropy and magnetization jumps (cf. Fig. 1). The opposite signs of the magnetization jumps $\Delta M(B\|a)$ and $\Delta M(B\|b)$ observed in small magnetic fields already imply that the phase boundaries originating at T_{SR} exhibit opposite slopes dB_C/dT. For a discontinuous phase transition, the slope of the phase boundary

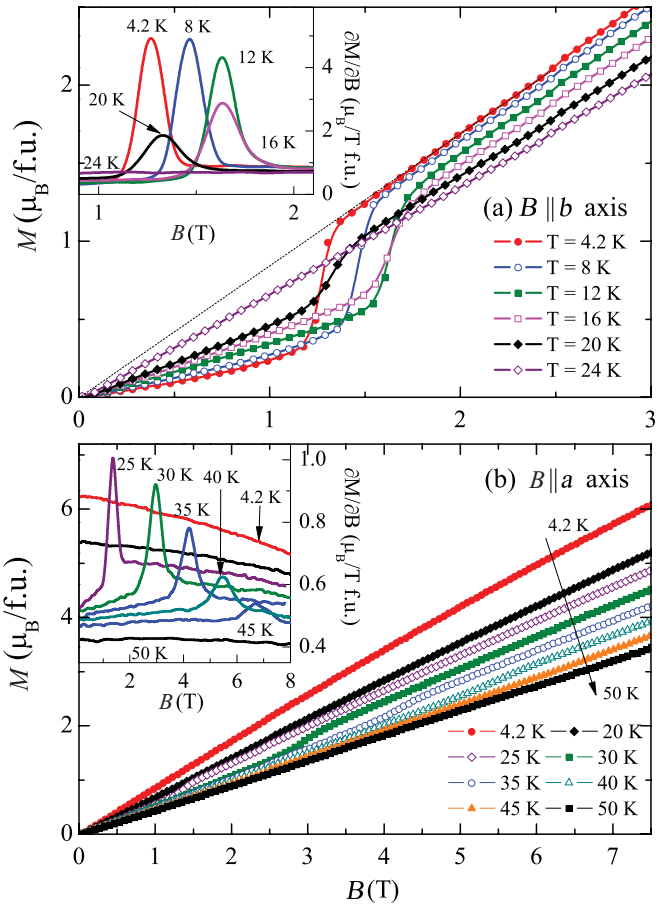

FIG. 4. (Color online) Field dependence of the magnetization (a) $M_b(B)$ in magnetic fields up to $B = 3$ $T \parallel b$ and (b) $M_a(B)$ in magnetic fields up to $B = 8$ $T \parallel a$ at different temperatures in the antiferromagnetically ordered phase (note: $T_{SR} = 23$ K). Inset: Derivatives $\partial M/\partial B$.

is associated with the ratio of the entropy changes ΔS and the magnetization changes ΔM at the phase transition according

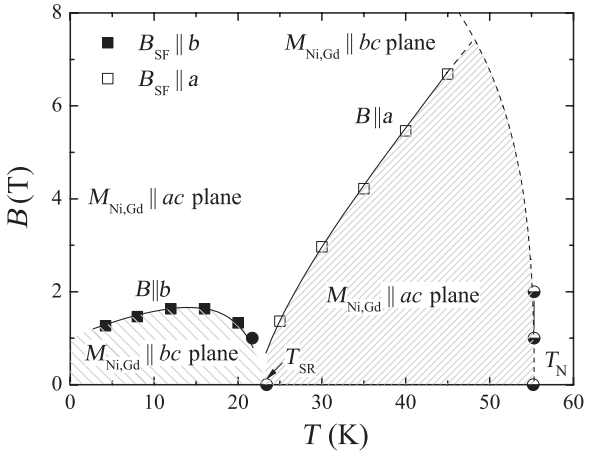

FIG. 5. Magnetic phase diagram constructed from the magnetization data and specific heat data. Open (filled) squares denote the spin-reorientation fields B_C as extracted from $M(B\|a)$ ($M(B\|b)$) measurements; cycles label the antiferromagnetic ordering temperature T_N and the spin-reorientation temperature T_{SR} from specific heat data. Lines are guides to the eyes.

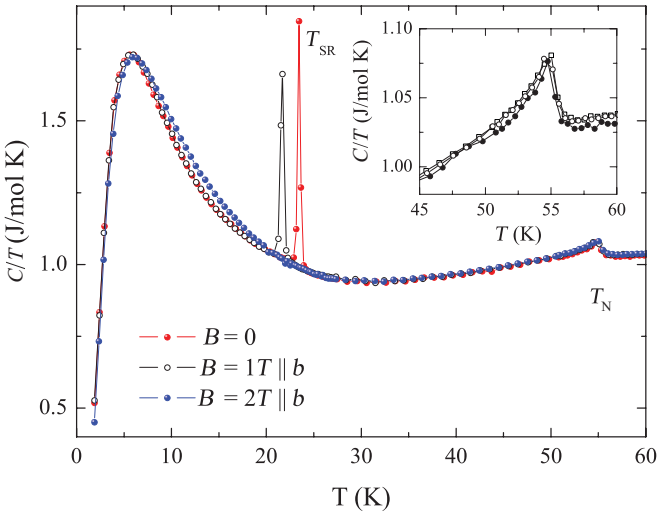

FIG. 6. (Color online) Temperature dependence of the specific heat $C(T, B)/T$ at $B = 0$, $B = 1\ T \parallel b$ axis, and $B = 2\ T \parallel b$ axis. The inset highlights the antiferromagnetic transition.

to $dB/dT = -\Delta S/\Delta M$ (Clausius–Clapeyron relation).[22] Our experimental data presented previously hence allow us to calculate the initial slopes of the phase boundaries at T_{SR}, i.e., $dB_{\parallel b}/dT = -7.1$ T/K and $dB_{\parallel b}/dT = 10.5$ T/K. Interestingly, the strong specific heat discontinuity at the phase boundary vanishes in external magnetic fields $B \parallel a = 2$ T (Fig. 6). In contrast, although magnetic fields $B \parallel b$ suppress the phase transition, the pronounced entropy jump is preserved, as evidenced by a strong peak in the specific heat (Fig. 6). Note that the flat slope of the phase boundary suggests negligible magnetization changes $\Delta M(B \parallel b) \sim 0$ if T_{SR} is suppressed down to ~15 K and $\Delta M(B \parallel b) < 0$ at lower temperatures.

III. DISCUSSION

Gd_2BaNiO_5 contains two kinds of magnetic ions, i.e., Ni^{2+} ($S = 1$) and Gd^{3+} ($S = 7/2$, $L = 0$) ions, which in general govern its magnetic properties. At high temperatures, however, the magnetic susceptibility is described by the Gd^{3+}-paramagnetism. The susceptibility data, above $T = 100$ K, are well described by the Curie-Weiss law with the Weiss temperature $\Theta \approx -13$ K and the effective magnetic moment $\mu_{eff} = 11.17\ \mu_B$. The negative value of Θ points to predominance of antiferromagnetic exchange interactions. The value of μ_{eff} is very close to the free-ion value for the Gd^{3+}-ion of $\mu_{eff} = 11.22\ \mu_B$ (note the two gadolinium ions per f.u. in Gd_2BaNiO_5). On the other hand, the theoretical effective moment amounts to $\mu_{eff} = 11.58\ \mu_B$ if spin $S = 1$ of the Ni^{2+}-ion is taken into account, which contradicts the experimental data. This indicates that the Ni subsystem only contributes negligibly to the magnetic susceptibility in this temperature range, which agrees to studies on the isostructural compound Y_2BaNiO_5 where the magnetic susceptibility is very small and exhibits a maximum at room temperature, indicating the Haldane gap state.[23] The value of this maximum is much less (by a factor of 1000) than the susceptibility of Gd_2BaNiO_5. We hence may conclude that the Haldane gap state is preserved in Gd_2BaNiO_5 at high temperatures. This assumption is supported by the observation of an energy gap in the magnetic excitation spectrum of about 11 meV in R_2BaNiO_5 with R = Pr, Nd, above the magnetic ordering temperature of these compounds.[8,11]

As previously mentioned, it is reported that the magnetically ordered phases of Nd_2BaNiO_5 and Pr_2BaNiO_5 coexist with the Haldane gap state of the Ni chains.[8,11] In this situation it is not *a priori* clear whether at all or to which extent the Ni subsystem exhibits isotropic susceptibility exponentially decreasing to zero at low temperatures typical for the quasi-1D $S = 1$ Heisenberg antiferromagnet or whether it shows anisotropic magnetic properties similar to a classical antiferromagnet. In order to extract this information from the experimental data presented above, the magnetic response of the Gd subsystem to the total magnetization and specific heat of Gd_2BaNiO_5 should be estimated. It is governed by the low-lying Gd^{3+}-crystal field levels split in the effective magnetic field resulting from both the external and internal fields. We conclude from neutron scattering experiments on other compounds of the family R_2BaNiO_5,[11–13] that both magnetic subsystems—the Ni and the Gd one—can be considered as two interacting sublattices of which orientation of magnetic moments can be read from the magnetization data.

The sharp jump in the magnetization curve as well as the linear dependence of $M(B)$ at $B > B_C$, which can be interpolated to zero at $B = 0$ (cf. Figs. 3 and 4), are typical for an uniaxial antiferromagnet magnetized along the easy axis. The data imply that a spin-flop transitions occurs in magnetic fields $B \parallel b$ axis at $T < T_{SR} = 24$ K and above this temperature when $B \parallel a$ axis. The appearance of a spin-flop transition for $B \parallel b$ and the observation of a significant decrease of $M_b(T)$ upon cooling below T_{SR} strongly suggest that the magnetic moments of both the Gd^{3+}- and the Ni^{2+}-ions are arranged in the bc plane at $T < T_{SR}$ and in small magnetic fields (see Fig. 6). Applying magnetic fields along the b axis causes a flop of the magnetic moments into the ac plane at a critical field B_C. The closer inspection of $M_b(T)$ reveals a positive curvature just below T_{SR}. Concomitantly, the specific heat data exhibit a Schottky-like feature, which will be discussed quantitatively below. Qualitatively, the Schottky anomaly is associated with a temperature-driven repopulation of the ground state sublevels of the Gd^{3+} ions, which is expected to show up in the magnetization, too. Indeed, the positive curvature in the magnetization data can be straightforwardly associated with such a Schottky-type anomaly. Note that a finite value of M_b at the lowest temperature possibly points to a small deviation of the nickel moments from the b axis.

The phase diagram in Fig. 5 summarizes the effect of external magnetic fields and temperatures. At $T < T_{SR}$ and either $B \parallel b < B_C$ or $B \perp b$, the Gd^{3+}- and Ni^{2+}-moments lie in the bc plane while they are arranged within the ac plane above T_{SR} and $B \parallel a < B_C$ or $B \perp a$. Applying a magnetic field perpendicular to the respective easy magnetic axis causes canting of the moments without anomalies in the magnetization curves $M(B)$ in the investigated field range until eventually in very high fields the full alignment of the moments is expected. Applying magnetic fields along the easy magnetic axis—the direction of which depends on temperature—yields a spin-flop transition which results in a

situation with perpendicular fields and canting of spins, as mentioned before.

Upon heating, the diminishing of the difference between transverse and longitudinal susceptibility should cause an increase of the spin-flop field and a decrease of the associated magnetization jump. This is indeed observed at very low temperatures as well as above T_{SR}. At $T > T_{SR}$ and $T < 14$ K, the spin-flop field shifts gradually to higher fields with increasing temperature. In contrast, below T_{SR}, there is a region of the phase diagram between $T \approx 14$ K and T_{SR} where $dB_C/dT < 0$. This behavior is caused by the shift of the spin-reorientational phase transition to lower temperature in applied external magnetic fields $B \parallel b$. Qualitatively, magnetic fields parallel to the b axis stabilize the magnetic structure with magnetization vector aligned along the b axis and hence shift the spin-reorientational transition to lower temperatures, which causes the experimentally observed nonmonotonous temperature dependence of B_C.

In order to estimate the contribution of the Gd subsystem to the magnetization and the specific heat below T_N, one has to consider the splitting of the Gd^{3+} ground state. The Gd^{3+} ions occupy a C_{2v} symmetry position. The effective magnetic field B_{eff} acting on the Gd^{3+}-ions results from both the external field B and the internal field B_{ex}, which mainly arises from the Ni subsystem due to f-d interaction. In addition, the Gd-Gd interaction has to be taken into account. B_{eff} splits the Gd^{3+} ground state into $2S + 1 = 8$ sublevels. The energies of these sublevels can be written as

$$E = \pm\tfrac{1}{2} n \Delta_{1,2}, \tag{1}$$

$$\Delta_{1,2} = g\sqrt{B^2_{\mathrm{eff}1,2\mathrm{a}} + B^2_{\mathrm{eff}1,2\mathrm{b}} + B^2_{\mathrm{eff}1,2\mathrm{c}}}\,\mu_B, \tag{2}$$

where $n = 1$, 3, 5, and 7. Here, we assume $g = 2$ for the all components $g_a = g_b = g_c = g$ of the g factor of the Gd^{3+}-ion. $B_{\mathrm{eff}1,2\alpha}$ ($\alpha = a, b, c$) are the components of the effective magnetic field. The indices 1 and 2 represent the Gd sublattices, named first and second sublattices, for which the component of the field created by the Ni subsystem $B_{ex\alpha}$ is oriented along or opposite to the direction of the external field B, respectively. Below T_N, Gd^{3+}-ions with opposite directions of the magnetic moments are not equivalent in the presence of external magnetic field $B \parallel \alpha$, and the effective fields acting on the Gd^{3+}-ions read

$$\begin{aligned} B_{\mathrm{eff}1\alpha} &= B + \kappa_{11\alpha} M^{\mathrm{Gd}}_{1\alpha} + \kappa_{12\alpha} M^{\mathrm{Gd}}_{2\alpha} + B_{ex\alpha} \\ B_{\mathrm{eff}2\alpha} &= B + \kappa_{11\alpha} M^{\mathrm{Gd}}_{2\alpha} + \kappa_{12\alpha} M^{\mathrm{Gd}}_{1\alpha} - B_{ex\alpha}. \end{aligned} \tag{3}$$

Here, $M^{\mathrm{Gd}}_{1\alpha}$ and $M^{\mathrm{Gd}}_{2\alpha}$ are the components of the magnetic moments of the first and second Gd sublattices, respectively. The parameters κ_{11} and κ_{12} determine the internal magnetic fields acting on the Gd^{3+}-ion with the magnetic moments, which are induced by Gd^{3+} ions with the same (κ_{11}) and opposite (κ_{12}) directions of their magnetic moments. Expanding the magnetic moments of gadolinium ions $M^{\mathrm{Gd}}_{1,2\alpha}$ in the effective magnetic fields [Eq. (3)] in powers of the differences $(B_{\mathrm{eff}1\alpha} - (B + B_{ex\alpha}))$ and $(B_{\mathrm{eff}2\alpha} - (B - B_{ex\alpha}))$ for the first and second Gd sublattices, respectively, we obtain the components of the magnetic moments:

$$M^{\mathrm{Gd}}_{1\alpha} = \frac{M^-_{0\alpha}\kappa_{12\alpha}\chi^+_{\alpha\alpha} + M^+_{0\alpha}(1 - \kappa_{11\alpha}\chi^-_{\alpha\alpha})}{(1 - \kappa_{11\alpha}\chi^-_{\alpha\alpha})(1 - \kappa_{11\alpha}\chi^+_{\alpha\alpha}) - \kappa^2_{12\alpha}\chi^-_{\alpha\alpha}\chi^+_{\alpha\alpha}} \tag{4}$$

$$M^{\mathrm{Gd}}_{2\alpha} = \frac{M^+_{0\alpha}\kappa_{12\alpha}\chi^-_{\alpha\alpha} + M^-_{0\alpha}(1 - \kappa_{11\alpha}\chi^+_{\alpha\alpha})}{(1 - \kappa_{11\alpha}\chi^-_{\alpha\alpha})(1 - \kappa_{11\alpha}\chi^+_{\alpha\alpha}) - \kappa^2_{12\alpha}\chi^-_{\alpha\alpha}\chi^+_{\alpha\alpha}}. \tag{5}$$

Here, $M^{\pm}_{0\alpha}$ and $\chi^{\pm}_{\alpha\alpha}$ are the components of the magnetic moments and magnetic susceptibility, respectively, in the effective field $\vec{B}_{\mathrm{eff}} = \vec{B} + \vec{B}_{ex}$. The "+" sign relates to the first Gd sublattice, the "−" one to the second sublattice. $M^{\pm}_{0\alpha}$ is calculated by differentiating Eq. (1) with respect to the components of the effective magnetic field assuming the Boltzmann distribution of electrons on the energy sublevels of Gd^{3+} ion:

$$M^{\pm}_{0\alpha} = 2\frac{g^2 B_{\mathrm{eff}\alpha}\mu^2_B}{\Delta_{1,2}}\left[4\mathrm{cth}\left(\frac{4\Delta_{1,2}}{kT}\right) - 0.5\mathrm{cth}\left(\frac{\Delta_{1,2}}{2kT}\right)\right], \tag{6}$$

where k is the Boltzmann constant. The factor 2 reflects the fact that the formula unit contains two gadolinium ions. Here, the splittings $\Delta_{1,2}$ are calculated from Eq. (2) using appropriate values of B_{eff}. Thereby, in the case of $B \parallel a$ axis, the components of the effective field are $B_{\mathrm{eff\,a}} = B \pm B_{\mathrm{ex\,a}}$; $B_{\mathrm{eff\,b}} = \pm B_{\mathrm{ex\,b}}$; and $B_{\mathrm{eff\,z}} = \pm B_{\mathrm{ex\,c}}$. Analogous expressions can be derived for other directions of the external magnetic field. The components of the magnetic susceptibility are calculated by differentiating (6) with respect to the external magnetic field, $\chi^{\pm}_{\alpha\alpha} = \frac{dM^{\pm}_{0\alpha}}{dB}|_{\vec{B}_{\mathrm{eff}} = \vec{B} + \vec{B}_{ex}}$. The components of the total magnetization can be described as a superposition of two contributions, $M_\alpha = 0.5(M_{1\alpha} + M_{2\alpha})$, where each contribution corresponds to one of the two Gd sublattices with appropriate B_{eff}.

As mentioned previously, the Schottky anomaly observed in the specific heat $C(T)$ reveals the temperature-driven repopulation of the ground state sublevels of the Gd^{3+}-ion. In terms of the two Gd sublattices this contribution can be written as

$$C_{1,2} = 2\mathrm{R}\left(\frac{\Delta_{1,2}}{kT}\right)^2 \left(\frac{1}{4\mathrm{sh}^2\left(\frac{\Delta_{1,2}}{2kT}\right)} - \frac{16}{\mathrm{sh}^2\left(\frac{4\Delta_{1,2}}{kT}\right)}\right), \tag{7}$$

where R is the gas constant.

In accordance with Eqs. (4)–(7), the contributions of the Gd subsystem to specific heat $C(T, B = 0)$ and magnetization $M_a(T)$, $M_b(T)$, and $M_c(T)$ were calculated varying the parameters κ_{11}, κ_{12}, $B_{ex}(T)$ as well as the angles between the nickel magnetic moments and crystallographic axes. The fitting curves thus obtained independently for $T < T_{SR}$ and $T_{SR} < T < T_N$ are shown by solid lines in Fig. 1. In the following the details of the fitting will be discussed.

The interactions between the Ni and the Gd subsystems are defined by the exchange field B_{ex}. We assume that the magnetic field B_{ex} created by the nickel subsystem is oriented along the direction of the nickel magnetic moment. In assumption of the temperature-independent angles α, β, and γ, between the directions of the magnetic moments of the Ni^{2+} ions and the a, b, and c axes of the crystal, respectively, we obtain $\alpha_1 = 90°$, $\beta_1 = 8.5°$, $\gamma_1 = 81.5°$ at $T < T_{SR}$, and $\alpha_2 = 14°$, $\beta_2 = 90°$, $\gamma_2 = 76°$ at $T_{SR} < T < T_N$. The value of the magnetic field B_{ex}

TABLE I. The κ_{11} and κ_{12} parameters of Gd-Gd interactions in various magnetic phases of Gd_2BaNiO_5.

	$T < T_{SR}$			$T_{SR} < T < T_N$		
α	a	b	c	a	b	c
$\kappa_{11\alpha}$ (G^2 mol/erg)	− 0.32	− 0.305	− 0.2	− 0.52	− 0.45	− 0.21
$\kappa_{12\alpha}$ (G^2 mol/erg)	− 0.4	− 0.126	− 0.4	− 0.13	− 0.3	− 0.42
$\kappa_{11\alpha}$ (G^2 mol/erg) flop-phase	− 0.36	− 0.3	− 0.21			
$\kappa_{12\alpha}$ (G^2 mol/erg) flop-phase	− 0.22	− 0.3	− 0.42			

is proportional to the nickel magnetic moment. This notion is supported by the observation that the splitting $\Delta(T)$ of the Er^{3+} ground doublet in the analogous compound Er_2BaNiO_5, measured by infrared spectroscopy,[24] is proportional to the magnetic moment $M_{Ni}(T)$ of the nickel subsystem measured by neutron diffraction.[25] In the case of Gd_2BaNiO_5, no temperature dependence of the nickel magnetic moments has been observed. We mention that the decrease of the magnetic field B_{ex} at increasing temperature up to T_N has been taken into account in the form $B_{ex}(T) = \frac{P_1}{P_2+\exp(P_3(T-P_4))}$, similar to an expression given in Ref. 7. Here, P_1, P_2, P_3, and P_4 are fitting parameters. The fitted $B_{ex}(T)$ curve shown in the inset to Fig. 2 has a kink at the temperature of the spontaneous spin-reorientational phase transition. The value of the magnetic field B_{ex} depends on the angle between the directions of the magnetic moments of Gd^{3+} and Ni^{2+} ions due to Ising type of the interaction.[26] The kink in the $B_{ex}(T)$ dependence at $T = T_{SR}$ manifests the different orientations of the magnetic moments of the Gd^{3+} ions with respect to the nickel magnetic moments below and above T_{SR}. If one neglects the Gd-Gd interactions, i.e., $\kappa_{11} = \kappa_{12} = 0$, the calculated Gd contribution to the magnetic susceptibility considerably exceeds the experimental results, as shown in Fig. 2 by solid lines. Therefore, the Gd-Gd interactions are mandatory to be included. The values of the fitted parameters κ_{11} and κ_{12} shown in Table I are close to $\kappa_{11} = \kappa_{12} = -0.0451\ T/\mu_B = -0.081\ G^2$ mol/erg estimated for polycrystalline Er_2BaNiO_5.[19] The difference between κ_{11} and κ_{12}, as given in Table I, could be ascribed to the difference in the exchange pathways. The values of κ_{11} and κ_{12} parameters change at the spin reorientation and the spin-flop transitions. Tentatively, this change may be ascribed to the fact that the Gd-Gd interaction is organized via Ni chains being therefore sensitive to the angle between Gd and Ni magnetic moments.

All fitted parameters κ_{11}, κ_{12}, $B_{ex}(T)$, and angles α, β, and γ were used for calculation of the gadolinium contribution to the magnetization $M(B)$, represented by solid lines in Fig. 3. In addition, the value of B_{ex} estimated from the fitting procedure allows us to explain the shift of the Schottky anomaly in $C(T, B)$ to higher temperature in a magnetic field $B \parallel b = 2$ T, as visible in Fig. 6. As has already been mentioned, below T_{SR} the magnetic moments of the Gd^{3+} ions lie in the bc plane. In zero external magnetic field $B = 0$ the effective magnetic fields calculated with Eq. (2) are roughly the same for both, i.e., the first and second Gd sublattices because the magnetic field created by the gadolinium sublattices $B_{Gd-Gd} \approx 0.2$ T is very small compared with the magnetic field created by the nickel subsystem $B_{ex} \approx 12$ T. However, in an applied field $B = 1$ T ($B \parallel b$ axis) the gadolinium contribution to the specific heat is different for the two Gd sublattices. For the Gd sublattice with magnetic moment projections opposed to the external magnetic field direction, the magnetic field leads to a decrease of the splitting of the ground state of the Gd^{3+} ion, and the Schottky anomaly shifts to lower temperatures. For the other Gd sublattice, the splitting increases, and the Schottky anomaly appears at higher temperatures. However, the total contribution of the two Gd sublattices does not lead to a shift of the Schottky anomaly because external magnetic field $B = 1$ T is again small compared with B_{ex}. When the system is in the flop phase, the magnetic moments of Gd^{3+} ions are perpendicular to the external magnetic field direction. In this case, both Gd sublattices give absolutely equal contributions to the specific heat. The magnetic field leads to an increase of the splitting, and the Schottky anomaly shifts to higher temperatures, as it is observed in experiment (cf. Fig. 6).

The difference $[M_\alpha - M_\alpha{}^{Gd}](T)$ of the experimental data and the calculated Gd-contribution is mainly due to magnetic susceptibility of the Ni ions. In the temperature range $T_{SR} < T < T_N$, the magnetic susceptibility along the different crystal directions is reasonably well described by the contribution of the Gd subsystem only, while the contribution of the Ni subsystem is negligible within the limits of the experimental error bars (cf. Fig. 1). Below T_{SR}, however, this difference implies a more complex behavior. The difference $[M_\alpha - M_\alpha{}^{Gd}](T)$ does not vanish at lowest temperatures, and it has the same value for different directions. Such behavior of the nickel subsystem indeed differs from that of a classical antiferromagnet. This behavior cannot be explained by paramagnetic impurities, which should give a Curie-like contribution to the magnetization $M(T)$. However, the experimental data exhibit clear kinks in $M_a(T)$ and $M_b(T)$ at $T = 7$ K while there is no anomaly in the specific heat data indicating a phase transition at this temperature. The magnetization $M(T)$ of the Haldane gap system, as known, should exhibit isotropic exponential decrease to zero at low temperatures. At present, however, there is no description of the temperature dependence $M(T)$

for the Haldane gap system in staggered magnetic field acting from the R subsystem.

IV. CONCLUSIONS

The thermodynamic properties of Gd_2BaNiO_5 single crystal are investigated by specific heat and magnetization measurements. Antiferromagnetic and spontaneous spin-reorientational phase transitions take place at $T_N = 55$ K and at $T_{SR} = 24$ K, respectively. The Gd-Gd interaction is organized via Ni chains being therefore sensitive to the angle between Gd and Ni magnetic moments. Below T_{SR}, the magnetic moments of both Ni^{2+} and Gd^{3+} ions lie in the bc plane of the crystal, and they flop to the ac plane under external magnetic field $B \parallel b$ axis. At $T_{SR} < T < T_N$, the magnetic moments flop from the ac to the bc plane. The anisotropic magnetic phase diagram in Gd_2BaNiO_5 is established from the experimental data. Considering the Gd-Gd and the Gd-Ni interactions allows estimating the contribution of the gadolinium subsystem to the magnetization and the specific heat and hence to discuss the Ni subsystem separately. Our analysis implies that the behavior of the nickel subsystem indeed differs from that of a classical antiferromagnet, and in particular our data suggest a gapped state of the Ni subsystem at low temperatures.

ACKNOWLEDGMENTS

The authors thank Guy Dhalenne and Pauline Higel for the growth of Gd_2BaNiO_5 single crystals. R.K., N.T., and B.B. acknowledge support from the D.F.G. via KL 1824/2. A.N.V. acknowledge support from Russian Ministry of Science and Education through State Contract 11.519.11.6012.

*Corresponding author: vasil@lt.phys.msu.ru

[1] F. D. M. Haldane, Phys. Lett. A **93**, 464 (1983); Phys. Rev. Lett. **50**, 1153 (1983).
[2] I. Affleck, J. Phys.: Condens. Matter **1**, 3047 (1989).
[3] A. Zheludev, S. Maslov, T. Yokoo, S. Raymond, S. E. Nagler, and J. Akimitsu, J. Phys.: Condens. Matter **13**, R525 (2001).
[4] K. Kojima, A. Keren, L. P. Le, G. M. Luke, B. Nachumi, W. D. Wu, Y. J. Uemura, K. Kiyono, S. Miyasaka, H. Takagi, and S. Uchida, Phys. Rev. Lett. **74**, 3471 (1995).
[5] R. Sáez-Puche, J. M. Corondo, C. L. Otero-Díaz, and J. M. Martín-Llorente, J. Solid State Chem. **93**, 461 (1991).
[6] J. Darriet and L. P. Regnault, Solid State Commun. **86**, 409 (1993).
[7] E. García-Matres, J. L. Garcia-Muñoz, J. L. Martínez, and J. Rodríguez-Carvajal, J. Magn. Magn. Mater. **149**, 363 (1995).
[8] A. Zheludev, J. M. Tranquada, T. Vogt, and D. J. Buttrey, Europhys. Lett. **35**, 385 (1996).
[9] V. Sachan, D. J. Buttrey, J. M. Tranquada, and G. Shirane, Phys. Rev. B **49**, 9658 (1994).
[10] E. A. Popova, D. V. Volkov, A. N. Vasiliev, A. A. Demidov, N. P. Kolmakova, I. A. Gudim, L. N. Bezmaternykh, N. Tristan, Y. Skourski, B. Büchner, C. Hess, and R. Klingeler, Phys. Rev. B **75**, 224413 (2007).
[11] A. Zheludev, J. M. Tranquada, T. Vogt, and D. J. Buttrey, Phys. Rev. B **54**, 7210 (1996).
[12] S. Raymond, T. Yokoo, A. Zheludev, S. E. Nagler, A. Wildes, and J. Akimitsu, Phys. Rev. Lett. **82**, 2382 (1999).
[13] T. Yokoo, S. A. Raymond, A. Zheludev, S. Maslov, E. Ressouche, I. Zaliznyak, R. Erwin, M. Nakamura, and J. Akimitsu, Phys. Rev. B **58**, 14424 (1998).
[14] S. Schiffler and H. Müller-Buschbaum, Z. Anorg. Allg. Chem. **532**, 10 (1986).
[15] J. Amador, E. Gutiérrez Puebla, M. A. Monge, and I. Rasines, Solid State Ionics **32-33**, 123 (1989).
[16] M. N. Popova, I. V. Paukov, Yu. A. Hadjiiskii, and B. V. Mill, Phys. Lett. A **203**, 412 (1995).
[17] G. A. Stewart, S. J. Harker, M. Strecker, and G. Wortmann, Phys. Rev. B **61**, 6220 (2000).
[18] A. Butera, M. T. Causa, M. Tovar, S. B. Oseroff, and S.-W. Cheong, J. Magn. Magn. Mater. **140**, 1681 (1995).
[19] M. N. Popova, S. A. Klimin, P. Higel, and G. Dhalenne, Phys. Lett. A **354**, 487 (2006).
[20] R. Klingeler, B. Büchner, K.-Y. Choi, V. Kataev, U. Ammerahl, A. Revcolevschi, and J. Schnack, Phys. Rev. B **73**, 014426 (2006).
[21] A. Tari, *The Specific Heat of Matter at Low Temperatures* (Imperial College Press, London, 2003).
[22] A. H. Morrish, *The Physical Principles of Magnetism* (Wiley, New York, 1965).
[23] T. Yokoo, T. Sakaguchi, K. Kakurai, and J. Akimitsu, J. Phys. Soc. Jpn. **64**, 3651 (1995).
[24] M. N. Popova, S. A. Klimin, E. P. Chukalina, B. Z. Malkin, R. Z. Levitin, B. V. Mill, and E. Antic-Fidancev, Phys. Rev. B **68**, 155103 (2003).
[25] J. A. Alonso, J. Amador, J. L. Martínez, I. Rasines, J. Rodríguez-Carvajal, and R. Sáez-Puche, Solid State Commun. **76**, 467 (1990).
[26] T. Kennedy, J. Phys.: Condens. Matters **2**, 5737 (1990).